

# Predicting the Environmental Impact of Active Sonar

Alec J. Duncan, Robert D. McCauley, and Amos L. Maggi

*Centre for Marine Science and Technology, Curtin University of Technology, GPO Box U1987, Perth, WA 6845, Australia*

**Abstract.** The effect of active sonar on marine animals, particularly mammals, has become a hot topic in recent times. The Australian Environmental Protection and Biodiversity Conservation Act 1999 obligates Defence to avoid significant environmental impacts from Navy activities including those which produce underwater sound such as active sonar. It is in the interests of all parties that these effects be modeled accurately to facilitate both the quantitative evaluation of the consequences of any proposed sonar trials, and the identification of suitable mitigation procedures. This paper discusses the received signal parameters that are of importance when predicting the effect of sonar systems on marine animals and techniques for modeling both the expected values of these parameters and their statistical fluctuations.

## INTRODUCTION

Relationships between acoustic signal parameters and the effects of the signals on marine animals are still unclear, as practical and legal difficulties have led to a paucity of experimental data. In the case of marine mammals the similarities between the inner ear mechanisms and those of land mammals [1] leads to an expectation that similar signal parameters will be important in both cases. Consideration of the data that does exist for marine mammals [2] together with data for land animals [3] suggests that the total received energy is likely to be the most important parameter at long range because it determines the loudness of the sound perceived by the animal, and hence the likelihood of a behavioral response. By contrast, at short range the peak signal pressure is likely to be the most important parameter because, for the short bursts of sound typical of sonar systems, it determines the likelihood of physiological damage.

This paper considers methods for predicting these parameters for hull mounted and sonobuoy based active sonars, which generally operate in the frequency range 2.5 kHz to 10 kHz. These systems are capable of transmitting a variety of signal waveforms, but the two most common are the single frequency tone burst, used for initial detection and Doppler determination, and the swept frequency burst used for accurate ranging.

Sound propagation in the ocean is subject to random fluctuations due to the presence of inhomogeneities in the water column and interactions of the sound with the rough sea surface and seabed. When dealing with environmental impacts it is, therefore, desirable to determine the probability distributions of the signal parameters

of interest so that the probabilities of exceedence of appropriate thresholds can be computed.

The approach taken in the work described here was to simulate an ensemble of received signals for a typical scenario using a standard high frequency propagation model and the assumption of uncorrelated random fluctuations in the relative arrival times of signals that have traveled by the different ray paths. This was carried out for both a tone burst and a swept frequency signal. The statistics of the received signal energy and signal peak pressure were then computed and fitted to appropriate theoretical probability density functions.

## PREDICTION OF RECEIVED SIGNAL PARAMETERS

### Theory

The theory presented here is based on the assumption that samples of the envelope of the received signal can be treated as random variables with variance  $\mathbf{s}_x^2$  and a Rayleigh probability density function (pdf) [4]:

$$f_R(x) = \frac{x}{\mathbf{s}_x^2} e^{-\frac{x^2}{2\mathbf{s}_x^2}}. \quad (1)$$

The equation for this pdf, and the ones that follow, only apply to positive values of their arguments. They are implicitly assumed to be zero for negative arguments.

The samples are assumed correlated with an autocorrelation function that is zero for lags greater than  $\mathbf{t}_c$ . There are thus  $N = T_r/\mathbf{t}_c$  independent samples of the signal envelope available in a received signal of duration  $T_r$ .

### *Received energy*

The received energy is proportional to:

$$E = \int_0^{T_r} \frac{x(t)^2}{2} dt \approx \frac{T_r}{N} \sum_{i=1}^N \frac{x_i^2}{2} \quad (2)$$

where the  $x_i$  represent samples of the continuous time envelope function  $x(t)$ .

By using the usual rules for determining the probability distributions of functions of random variables [4,5] and assuming the samples are independent it is straightforward to show that  $y_i = x_i^2/2$  has an Exponential pdf:

$$f_e(y) = \frac{1}{\mathbf{s}_x^2} e^{-\frac{y}{\mathbf{s}_x^2}} \quad (3)$$

and that  $E$  has a Gamma pdf:

$$f_g(E) = \frac{E^{N-1}}{\mathbf{b}^N \Gamma(N)} e^{-E/\mathbf{b}} \quad (4)$$

with  $\mathbf{b} = \frac{\mathbf{s}_x^2 T_r}{N} = \mathbf{s}_x^2 \mathbf{t}_c$  and  $\Gamma(\cdot)$  representing the Gamma function.

The population mean and variance of  $E$  are:

$$\mathbf{m}_E = N\mathbf{b} = \mathbf{s}_x^2 T_r, \text{ and } \mathbf{s}_E^2 = N\mathbf{b}^2 = \frac{\mathbf{s}_x^4 T_r^2}{N}. \quad (5)$$

These equations can be combined to yield an expression for the number of independent samples:

$$N = \left( \frac{\mathbf{m}_E}{\mathbf{s}_E} \right)^2. \quad (6)$$

For sufficiently large  $N$  (say  $> 30$ ) the Central Limit Theorem will apply and the pdf of  $E$  will be well approximated by the Normal (Gaussian) pdf with the same mean and variance.

### *Peak pressure*

A pdf for the peak pressure can be derived by recognizing that for independent samples of the signal envelope the probability that the maximum of these samples,  $z = x_{\max}$ , is less than  $p$  is given by:

$$\int_0^p f_z(z) dz = \Pr(z < p) = \prod_{i=1}^N \Pr(x_i < p) = \left[ \int_0^p f_R(x) dx \right]^N. \quad (7)$$

Evaluating the expression on the right hand side of Equation (7) and differentiating with respect to  $p$  results in the following expression for the pdf of the maximum (peak) of the envelope:

$$f_z(z) = \frac{Nz}{\mathbf{s}_x^2} e^{-\frac{z^2}{2\mathbf{s}_x^2}} \left( 1 - e^{-\frac{z^2}{2\mathbf{s}_x^2}} \right)^{N-1} \quad (8)$$

### **Simulation of received signals**

The scenario considered here was a 150 m deep isovelocity water column, with a sound speed of  $1,500 \text{ m.s}^{-1}$  and a density of  $1,024 \text{ kg.m}^{-3}$ . The seabed was a fluid half-space with a sound speed of  $1,750 \text{ m.s}^{-1}$ , a density of  $1940 \text{ kg.m}^{-3}$ , and an attenuation of 0.8 dB per wavelength. The source depth was 6 m, the receiver depth 10 m, and the source to receiver range varied from 2 km to 3 km. Two transmit signals were considered: a tone burst with a frequency of 7.5 kHz, a duration of 1s, and a 10% cosine amplitude taper on each end; and a burst of the same duration and amplitude taper, but with a linear frequency sweep from 6.8 kHz to 8.2 kHz.

The Gaussian beam-tracing model Bellhop ([6], [7]), was used to determine the amplitudes and delays of the various arrivals, with only arrivals with amplitudes greater than one percent of the maximum being used in the received signal reconstruction. This resulted in 18 and 26 arrivals being summed at 2 km and 3 km range respectively. Received signals were generated by summing replicas of the

transmit signal delayed and scaled by the computed amounts. This process was carried out in the frequency domain so that phase shifts due to boundary reflections could be incorporated and the delays could be included without interpolation error. Different received signal realizations were obtained by perturbing the computed delays by random amounts prior to calculating the received signal. The perturbations were taken from a Gaussian random number generator with a standard deviation of  $200\ \mu\text{s}$ . A sensitivity test showed that the results were indistinguishable for perturbation standard deviations greater than a quarter of a period of the lowest frequency present ( $37\ \mu\text{s}$ ).

Envelopes for five realizations of the received signal for each transmit signal are shown in Fig 1. The received signals due to the different transmit signals have a very different character, with the swept frequency signal envelope having larger and more rapid fluctuations than the tone burst envelope, reflecting its much wider bandwidth.

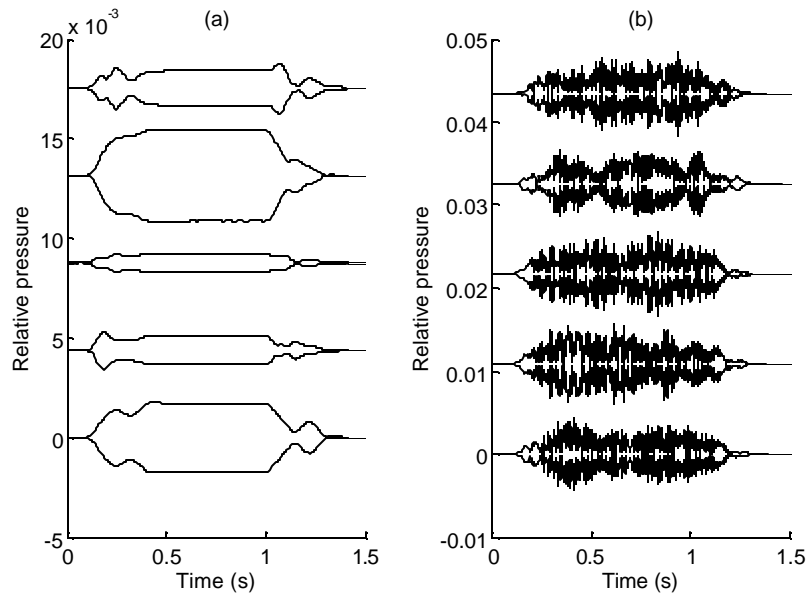


**FIGURE 1.** Envelopes of five realizations of the received signal for (a) tone burst and (b) frequency sweep.

## Results

Results are presented here for a receiver range of 2 km. Limited space precludes including the results for other ranges, which were qualitatively very similar to those presented here.

### *Received energy*

Figure 2 shows a comparison between the pdf of the received energy for the tone burst estimated from the simulation and the Gamma pdf with the same mean and standard deviation.

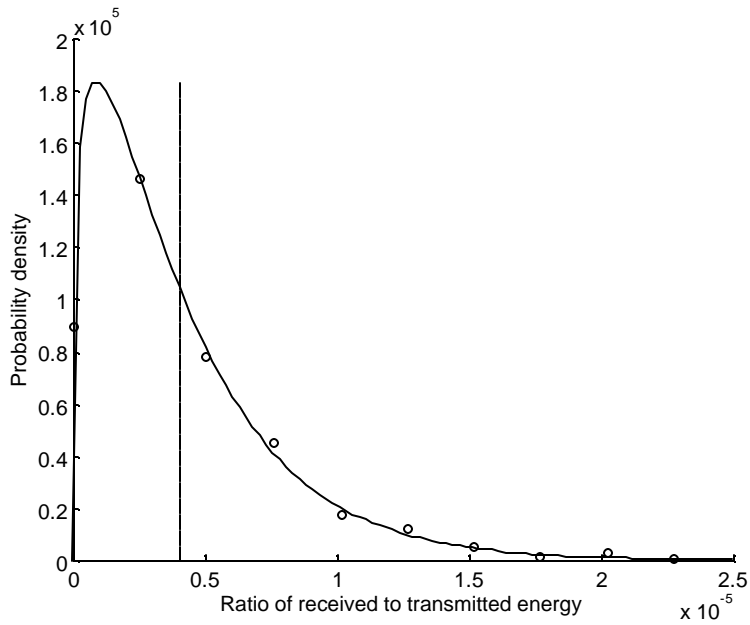


**FIGURE 2.** Circles are probability density of received energy estimated from 1000 signal realizations for tone burst signal. Solid line is gamma probability density function Equation (4) with  $m_E = 4.1 \times 10^{-6}$ ,  $s_E = 3.6 \times 10^{-6}$ . Vertical broken line is expected signal energy computed from the sum of the squares of the arrival amplitudes, vertical dotted line (indistinguishable from broken line) is mean energy of signal realizations.

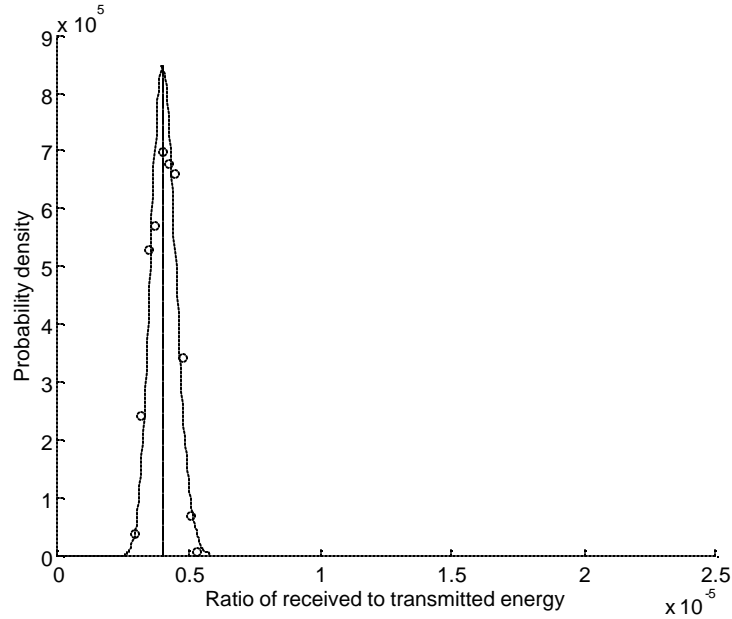


**FIGURE 3.** As for Figure 2, but swept frequency transmit signal.  $m_E = 4.1 \times 10^{-6}$ ,  $s_E = 4.7 \times 10^{-7}$ .

The equivalent plot for the swept frequency signal is shown in Fig 3. In each case, a histogram of the energies of 1,000 received signal realizations was calculated. This

was then normalized for comparison with the theoretical pdf by dividing by the product of the number of samples and the bin spacing.

In both cases the mean energy agreed with the value computed from the sum of the squares of the absolute values of the arrival amplitudes computed by Bellhop, but the tone burst produced a much greater spread in received energy than the sweep. This was a direct consequence of the wider bandwidth of the sweep, which resulted in a shorter envelope correlation time and, therefore, a greater number of independent samples being available in each receive signal. The values of  $\mathbf{s}_x$  and  $N$  estimated from the data using Equations (5) and (6) are given in Table 1. To make subsequent comparisons easier, the tabulated values of  $\mathbf{s}_x$  have been renormalized relative to the peak pressure of the transmit signal,  $z_{Tx}$ , rather than the transmit energy,  $E_{Tx}$ , by multiplying the values calculated using Equation (5) by a factor of  $\sqrt{E_{Tx}}/z_{Tx}$ .

**TABLE 1.** Fitted signal parameters

Estimated Using	Normalized Envelope Standard Deviation, $\mathbf{s}_x$	Number of independent samples, $N$
Tone-burst, Energy Pdf	$1.4 \times 10^{-3}$	1.3
Tone-burst, Peak Pdf	$1.3 \times 10^{-3}$	2.0
Sweep, Energy Pdf	$1.4 \times 10^{-3}$	73
Sweep, Peak Pdf	$1.4 \times 10^{-3}$	258

### *Peak pressure*

Similar results for the pdfs of the peak received signal pressures are shown in Figs 4 and 5. Here the incoherent sum of the arrival amplitudes gives a reasonable estimate of the mean value of the signal peak for the tone-burst, but underestimates it by a factor of 2.5 (8dB) for the sweep. The theoretical pdf given by Equation (4) provides a good fit to the data for both signal types when the parameters are adjusted to minimize the least square error. The fitted envelope standard deviations agree with those calculated using the energy pdfs but the numbers of independent samples differ (Table 1).

Note that the pdfs are clearly skewed, even for the sweep with 258 samples, demonstrating that the Central Limit Theorem does not apply in this case.

## DISCUSSION AND CONCLUSIONS

The probability density functions based on the simplifying assumptions of a Rayleigh pdf for the signal amplitude and statistically independent samples provided good fits to the simulation results.

The received energy pdfs for the tone burst and sweep had the same mean, which also agreed with the values computed via an incoherent transmission loss calculation. However, the energy pdf for the tone burst had a much higher standard deviation than that for the sweep, with a consequent higher probability of extreme values.

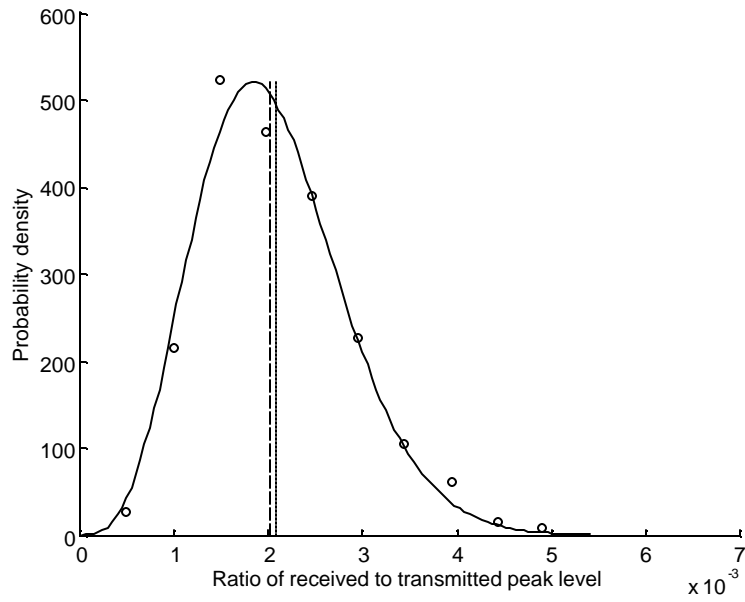


**FIGURE 4.** Circles are probability density of ratio of peak received pressure to peak transmit pressure estimated from 1,000 signal realizations for tone burst signal. Solid line is fitted theoretical probability density given by Equation (8) with  $s_x = 1.26 \times 10^{-3}$ ,  $N = 2.0$ . Vertical broken line is expected ratio computed from incoherent sum of arrival amplitudes, vertical dotted line is mean ratio of signal realizations.

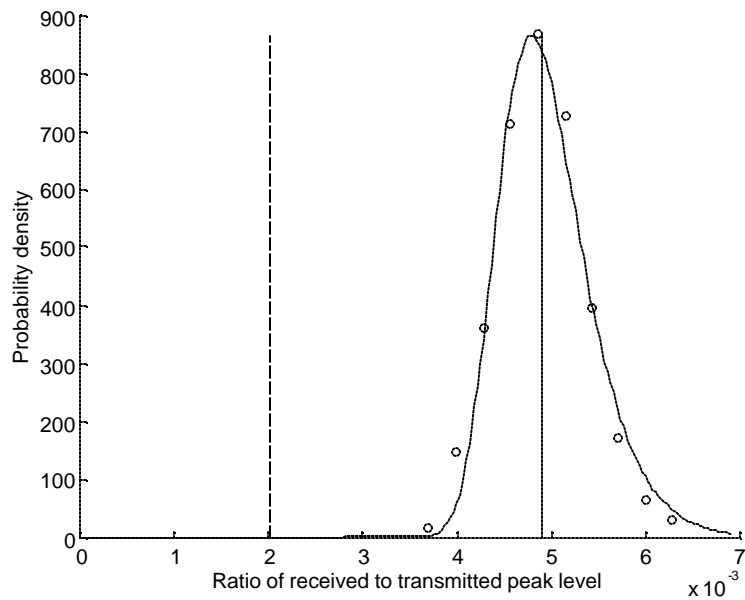


**FIGURE 5.** As for Figure 4, but swept frequency transmit signal.  $s_x = 1.43 \times 10^{-3}$ ,  $N = 258$ .

The peak signal pdf for the tone burst had a mean value close to the value expected from the incoherent transmission loss calculation, but the peak signal pdf for the sweep was shifted to right, with a mean corresponding to a transmission loss 8dB lower than the incoherent calculation. This is particularly significant in the context of estimating environmental impacts.

These effects are explained by the much wider bandwidth and hence shorter correlation time of the sweep compared to the tone burst, resulting in the sweep signal envelope having a larger number of independent samples than the tone burst envelope.

There was, however, quantitative disagreement between the numbers of independent samples estimated from the energy pdfs and those estimated from the peak pdfs (Table 1). This discrepancy was particularly apparent for the sweep signal and is likely to be due to a breakdown of the assumption that the received signal envelope can be treated as a random variable when there are a limited number of arrivals. The authors are investigating this further.

## ACKNOWLEDGMENTS

This work has been made possible by financial support provided by the Defence Science and Technology Organisation, Australia (DSTO).

## REFERENCES

1. Darlene R Ketten *Bioacoustics* **8**, 103 (1997).
2. James J Finneran, Carolyn E. Schlundt, Randall Dear, et al. *Journal of the Acoustical Society of America* **111** (6), 2929 (2002).
3. Robert Lataye and Pierre Campo *Journal of the Acoustical Society of America* **99** (3), 1621 (1996).
4. Alexander D. Poularikas, *The Handbook of Formulas and Tables for Signal Processing*. (CRC Press, 1999).
5. Ronald E. Walpole and Raymond H. Myers, *Probability and Statistics for Engineers and Scientists*, 3rd ed. (Macmillan, 1985).
6. Michael B Porter and Homer P. Bucker *Journal of the Acoustical Society of America* **82** (4), 1349 (1987).
7. Michael B Porter, Acoustic Toolbox (Atpii\_F95) (1999).